IEEE Access
Multidisciplinary | Rapid Review | Open Access Journal

Received March 26, 2021, accepted April 11, 2021, date of publication April 14, 2021, date of current version April 23, 2021.

Digital Object Identifier 10.1109/ACCESS.2021.3073173

Random Errors in Broadband Characterization of the Propagation Constant of Transmission Lines Using Multiple Two-Port Measurements

MARIO PÉREZ-ESCRIBANO, (Graduate Student Member, IEEE), AND ENRIQUE MÁRQUEZ-SEGURA, (Senior Member, IEEE)

Departamento de Ingeniería de Comunicaciones, Escuela Técnica Superior de Ingeniería de Telecomunicación, Universidad de Málaga, 29010 Málaga, Spain

Corresponding author: Mario Pérez-Escribano (mpe@ic.uma.es)

This work was supported in part by the Spanish Ministerio de Economía, Industria y Competitividad, under Grant ADDMATE TEC2016-76070-C3-3-R (AEI/FEDER, UE), in part by the Spanish Ministerio de Educación, Cultura y Deporte, under Grant FPU16/00246, and in part by the Universidad de Málaga, under I Plan Propio de Investigación y Transferencia (C.1).

ABSTRACT In this work, a comparison between three broadband methods used to estimate the propagation constant of planar transmission lines is presented. The goal of this comparison is to study how possible random measurement errors can affect the use of the aforementioned methods commonly used, since in ideal conditions the same solution is obtained from all of them. For this purpose, a sensitivity analysis is carried out in order to study the similarities and differences and how errors in measured S-parameters and in line lengths affect the attenuation and the phase constant obtained from each method. Subsequently, a minimization approach that consists of a least-square estimation using a criteria to choose the optimal line lengths is proposed to minimize measurement errors. Finally, an experiment has been designed, manufactured using microstrip transmission lines, and measured to validate the developed theory. Results corroborate the proposed theory and show an excellent agreement with electromagnetic simulations in the 0.1- to 50-GHz frequency band, therefore assessing the suitability of the proposed error analysis.

INDEX TERMS Attenuation constant, broadband measurements, characterization, error analysis, microstrip line, phase constant, propagation constant, random errors, transmission line measurements.

I. INTRODUCTION

The experimental determination of the propagation constant of planar transmission lines is extremely important in the design of microwave and millimeter-wave circuits. In recent years, the imminent arrival of new materials, such as printed materials, used to manufacture microwave circuits, several studies have been based on the measurement of the propagation constant to extract the electromagnetic properties of these materials [1]–[3]. The methods available to obtain the propagation constant can be classified into several categories depending on the sort of measurements considered [4]. The first possible classification distinguishes between broadband [5] and resonant methods [6]. On the one hand, the former methods allow the characterization of the propagation constant in a wide range of frequency points measured. Their main drawback can be the accuracy, that depends on the precision of the measurements, showing a worst behavior, precisely, at resonances. On the other hand, resonant methods allow an accurate estimation of the propagation constant in a discrete set of frequency points, those where a resonance on the test structure occurs. However, they cannot be useful when broadband characterization is required. From another point of view, another classification distinguishes between 1-port [7] and 2-port [8], [9] measurements.

This work deals precisely with 2-port measurement methods for general transmission lines. The propagation constant can be obtained, e.g., as a result of a TRL (Thru-Reflect-Line) calibration using two lines or more lines of different lengths [10]–[12]. Nevertheless, resonances due to that length differences can degrade the resulting curves. In this sense, several works have proposed improvements by increasing the number of lines, as in [13]. This strategy was used to define the multiline TRL calibration [11]. For this reason,

The associate editor coordinating the review of this manuscript and approving it for publication was Feng Lin.

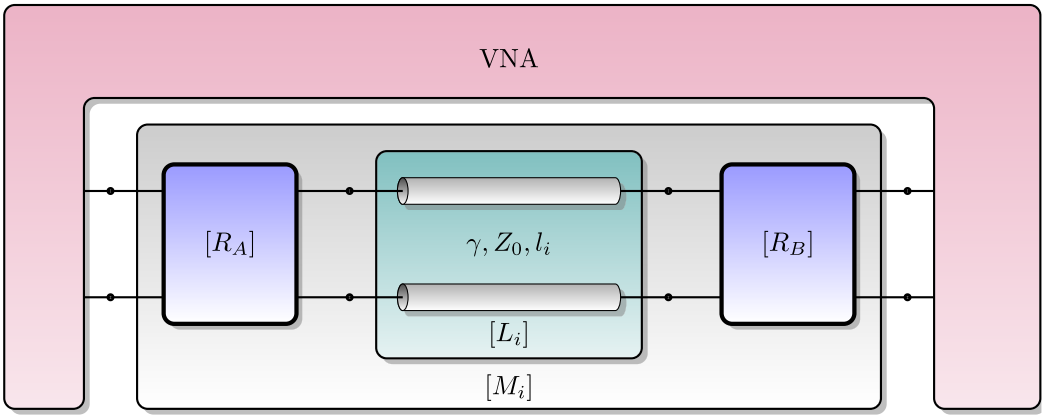

FIGURE 1. Measurement setup.

an over determination based on applying traditional methods and increasing the number of lines and choosing properly the length of the transmission lines is proposed in this paper.

As the aforementioned TRL method, there are different techniques based on invariant two-port [12], [14] that, in a first look, bear a strong resemblance between them. These several techniques for measuring the propagation constant have been examined, showing that ideally they are similar, but in the presence of measurement errors, their behavior is completely different. In this work, the interface between the Vector Network Analyzer (VNA) and the outer is a coaxial port, so some fixture between that terminal and the Line Under Test (LUT) must be included. The fixture produces a discontinuity in the signal path that strongly affects the measurement. The concept of algebraic invariant of networks in linear embedding is a common tool in the theory of linear active and non-reciprocal networks [15]. The use of an invariant allows the extraction of the effects of the test-fixture from the parameter estimated. This means that no VNA calibration is necessary when using at least two transmission lines measurements. This work deals with three different formulations for broadband methods using 2-port S-parameters. The main focus is on methods that use the invariant properties of similar matrix transformations. These methods avoid the systematic errors of other measurement techniques due to mismatching between the characteristic impedance of the VNA and the LUT using mathematical invariants. However, this behavior does not occur with random errors.

A study on how random errors affect broadband methods for the characterization of the propagation constant of transmission lines has been carried out. It is based on two-port measurements of transmission lines and it is required the use of a two-port VNA with no need of calibration. The three analyzed methods are described in Section II. In order to study how random errors affect each of the methods, a sensitivity analysis has been performed and the results are summarized in Section III. Section IV shows a technique to minimize errors, based on the over determination of the methods using a least-square estimation. The developed theory is corroborated through real measurements in Section V. Finally, conclusions are given in the last section.

II. DESCRIPTION OF THE METHODS

The methods treated in this work use a measurement setup as shown in Fig. 1. The two-port S-parameters of two lines with different lengths are measured and the transmission parameters matrices, $[M_1]$ and $[M_2]$, are calculated. The transmission matrices can be obtained easily from the measured S-parameters using the following expressions [16]:

$$T_{11} = \frac{1}{S_{21}} \quad T_{12} = -\frac{S_{22}}{S_{21}}$$
$$T_{21} = \frac{S_{11}}{S_{21}} \quad T_{22} = \frac{S_{12}S_{21} - S_{11}S_{22}}{S_{21}}. \tag{1}$$

According to Fig. 1, the measured cascade matrices of the two lines of different lengths can be written as $[M_1] = [R_A][L_1][R_B]$ and $[M_2] = [R_A][L_2][R_B]$. The matrices $[L_1]$ and $[L_2]$ are the transmission matrix of the lines measured excluding the transition between ports and the LUT, whose effects are considered in matrices R_A and R_B. The L_i matrices for every line measured are given by

$$[L_i] = \begin{bmatrix} e^{\gamma l_i} & 0 \\ 0 & e^{-\gamma l_i} \end{bmatrix}. \tag{2}$$

A. METHOD 1

The measured matrices can be combined in the following way

$$[M_1][M_2]^{-1} = [R_A][L_1][L_2]^{-1}[R_A]^{-1}. \tag{3}$$

Equation (3) is an eigenvalue equation that can be rewritten as $[M] = [R_A][L][R_A]^{-1}$, where $[M] = [M_1][M_2]^{-1}$ and $[L] = [L_1][L_2]^{-1}$. $[M]$ and $[L]$ are similar matrices and in consequence their eigenvalues, traces and determinants coincide. As $[L]$ is a diagonal matrix, $[L] = \text{diag}(e^{+\gamma\Delta l}, e^{-\gamma\Delta l})$, its eigenvalues are $e^{+\gamma\Delta l}$-and $e^{-\gamma\Delta l}$, respectively, and its trace is $e^{+\gamma\Delta l} + e^{-\gamma\Delta l}$. These values are the same for $[M]$. In order to obtain the propagation constant, the invariants mentioned above can be used. At this point, the three methods that will

be used to obtain the propagation constant must be defined. On the one hand, due to that trace does not change under a similarity transformation, the following equality holds

$$\text{trace}([L]) = \text{trace}([M]) = e^{-\gamma\Delta l} + e^{+\gamma\Delta l}, \tag{4}$$

being $\Delta l = l_2 - l_1$. Therefore, the propagation constant can be calculated as

$$\gamma = \frac{1}{\Delta l}\cosh^{-1}\left(\frac{\text{trace}\left([M_1]\,[M_2]^{-1}\right)}{2}\right). \tag{5}$$

B. METHOD 2

On the other hand, the eigenvalues of $[M]$ are identical to the eigenvalues of $[L]$. Therefore, if λ_1 and λ_2 are the eigenvalues of $[M]$, they must be equals to $e^{-\gamma\Delta l}$ and $e^{+\gamma\Delta l}$, respectively [17]. Solving these equations for γ, it is obtained

$$\gamma = \frac{1}{\Delta l}\ln\left(\frac{1}{\lambda_1}\right) = \frac{1}{\Delta l}\ln(\lambda_2). \tag{6}$$

In this case, two different values can be obtained for the propagation constant, and an average of the eigenvalues of $[M]$, $1/2\,(1/\lambda_1 + \lambda_2)$, can be used to calculate γ, that is

$$\gamma = \frac{1}{\Delta l}\ln\left(\frac{1/\lambda_1 + \lambda_2}{2}\right). \tag{7}$$

C. METHOD 3

Starting again in a different way [14], the sum of the measured matrices, $[M_{1+2}] = [M_1] + [M_2]$, instead of the product, can be considered and expressed as

$$[M_{1+2}] = R_A\begin{pmatrix} e^{+\gamma l_1}\left(1 + e^{+\gamma\Delta l}\right) & 0 \\ 0 & e^{-\gamma l_1}\left(1 + e^{-\gamma\Delta l}\right)\end{pmatrix}R_B. \tag{8}$$

Taking the determinant of the resulting matrix in Eq. (8) and dividing it by the determinant of $[M_1]$, the result is

$$\frac{\det([M_{1+2}])}{\det([M_1])} = \left(1 + e^{+\gamma\Delta l}\right)\left(1 + e^{-\gamma\Delta l}\right). \tag{9}$$

From Eq. (9), the propagation constant can be obtained as

$$\gamma = \frac{1}{\Delta l}\cosh^{-1}\left(\frac{\det([M_{1+2}])}{2\det([M_1])} - 1\right). \tag{10}$$

D. SIMPLIFIED EQUATIONS

As seen in the developed equations, port effects (R_A and R_B) has been removed from the formulas. For this reason, the methods will work in the same way with or without VNA calibration. All these mathematical expressions can be rewritten as a function of the measured S-Parameters instead of T-parameters to fulfill the later sensitivity analysis. They are shown in Appendix A. However, these complex equations can be quite simplified in case $Z_0 = Z_c$, because $S_{11}^{(n)}$ and $S_{22}^{(n)}$ can be taken as 0. Furthermore, as the lines are reciprocal devices, it must be fulfilled that $S_{21}^{(n)} = S_{12}^{(n)}$. Under these ideal conditions, Eqs. (29)-(31), as shown at the top of page 10, can be reduced to:

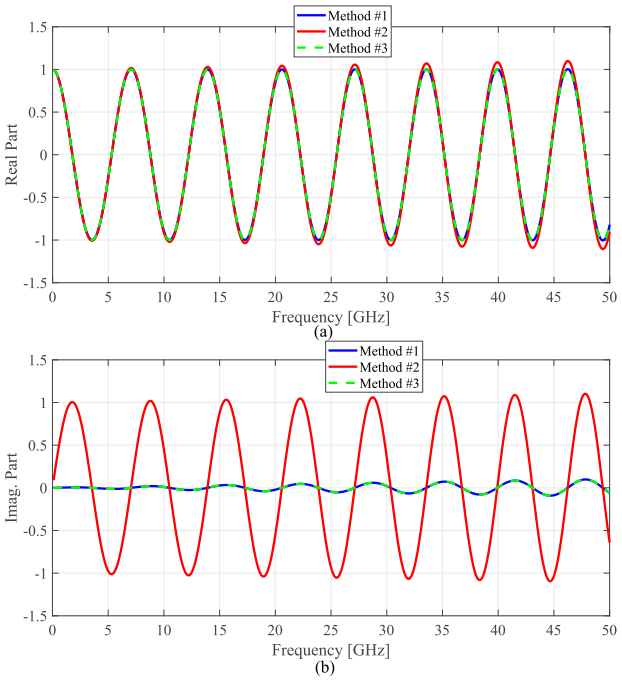

FIGURE 2. Real (a) and imaginary (b) parts of the argument of method functions.

1) Method 1:

$$\gamma = \frac{1}{\Delta l}\cosh^{-1}\left(\frac{\left(S_{21}^{(1)}\right)^2 + \left(S_{21}^{(2)}\right)^2}{2S_{21}^{(1)}S_{21}^{(2)}}\right). \tag{11}$$

2) Method 2:

$$\gamma = \frac{1}{\Delta l}\ln\left(\frac{S_{21}^{(2)}}{S_{21}^{(1)}}\right). \tag{12}$$

3) Method 3:

$$\gamma = \frac{1}{\Delta l}\cosh^{-1}\left(\frac{\left(S_{21}^{(1)} + S_{21}^{(2)}\right)^2}{2S_{21}^{(1)}S_{21}^{(2)}} - 1\right). \tag{13}$$

These simplified expressions are more practical than general case equations, and will be used in the sensibility analysis to extract the variances of α and β as a function of the S-parameters variances.

In order to evaluate the behavior of these methods, a simulation of two lines using Rogers 4350B substrate, with 30 mil thickness, $\varepsilon_r = 3.66$, $\tan\delta = 0.0031$, and 17.5 μm thick copper metallization. The line width is set to 1.65 mm, to get a 50 Ω characteristic impedance, whereas the lengths are 10 and 35 mm respectively. Figure 2 shows the real and imaginary part of z_i, being z_i the argument of $\cosh^{-1}$ or ln of the proposed methods ($i = 1, 2, 3$ indicates the method). As it is seen, Methods 1 and 3 works in a similar way, as (29) and (31) are exactly the same if operated in the ideal case, whereas imaginary part of the argument of Method 2 is completely different.

It is important to consider that z_i, the argument of method functions, is a complex number defined as $z_i = r_i e^{j\theta_i}$. $\cosh^{-1}$ can be rewritten as a logarithmic function given by

$$\cosh^{-1}(z_i) = \ln(z_i + \sqrt{z_i - 1}\sqrt{z_i + 1}). \tag{14}$$

Therefore, for every method, the propagation constant can be expressed always as a logarithmic function given by

$$\gamma = \frac{1}{\Delta l}\left[\ln(r_i) + j(\theta_i + 2n\pi)\right], \tag{15}$$

being

$$\begin{aligned} \alpha &= \frac{1}{\Delta l}\ln(r_i) \\ \beta &= \frac{1}{\Delta l}(\theta_i + 2n\pi). \end{aligned} \tag{16}$$

In the context of a transmission line, r_i and θ_i are the attenuation and the electrical length of a line section whose length is Δl. In this point, it is important to mention that the attenuation information depends exclusively on the absolute value of r_i, whereas β information is in θ_i. These expressions will be the starting point of the sensitivity analysis of the next section, to know how random errors affect the propagation constant. It is noteworthy that α has an unique solution as $r \in R$ whereas β has an infinite number of solutions. This fact will play a very important role in the implementation of the methods using numerical algorithms.

III. SENSITIVITY ANALYSIS

For the sensitivity analysis, two error sources are considered. They are errors in line lengths and in the argument of method functions. For this purpose, and looking for the covariance of α and β, the derivatives of (16) with respect to r, θ and Δl can be expressed as

$$\begin{aligned} \frac{\partial\alpha}{\partial r} &= \frac{1}{r\Delta l} \\ \frac{\partial\alpha}{\partial\theta} &= 0 \\ \frac{\partial\alpha}{\partial\Delta l} &= -\frac{\ln(r)}{\Delta l^2} = -\frac{\alpha}{\Delta l} \\ \frac{\partial\beta}{\partial r} &= 0 \\ \frac{\partial\beta}{\partial\theta} &= \frac{1}{\Delta l} \\ \frac{\partial\beta}{\partial\Delta l} &= -\frac{\theta}{\Delta l^2}. \end{aligned} \tag{17}$$

From these expressions, and assuming that there is no covariance between errors in the argument of method functions and in the line lengths, the variances of the attenuation and phase constants are given by

$$\begin{aligned} \sigma_\alpha^2 &= \left|\frac{\partial\alpha}{\partial\Delta l}\right|^2\sigma_{\Delta l}^2 + \left|\frac{\partial\alpha}{\partial r}\right|^2\sigma_r^2 \\ &= \left|\frac{\alpha}{\Delta l}\right|^2\sigma_{\Delta l}^2 + \left|\frac{1}{r\Delta l}\right|^2\sigma_r^2, \end{aligned} \tag{18}$$

$$\begin{aligned} \sigma_\beta^2 &= \left|\frac{\partial\beta}{\partial\Delta l}\right|^2\sigma_{\Delta l}^2 + \left|\frac{\partial\beta}{\partial\theta}\right|^2\sigma_\theta^2 \\ &= \left|\frac{\theta}{\Delta l^2}\right|^2\sigma_{\Delta l}^2 + \left|\frac{1}{\Delta l}\right|^2\sigma_\theta^2, \end{aligned} \tag{19}$$

respectively.

As seen in the developed expressions, choosing a bigger Δl is the simplest way of reducing α and β variances. However, r and θ are just the absolute value and the phase of the argument of method functions. What can be measured is the magnitude ($\sigma^2_{|S_{21}|}$) and phase ($\sigma^2_{\phi S_{21}}$) variances of the S-parameters, that are a characteristic of each VNA. Due to the complexity of the equations obtained, it is impractical to obtain an analytical solution for the variances in Eqs. (18), (19) as a function of $\sigma^2_{|S_{21}|}$ and phase $\sigma^2_{\phi S_{21}}$. However, for the ideal case of Method 2 shown in Eq. (12), σ_α^2 and the phase σ_β^2 can be expressed as

$$\sigma_\alpha^2 = \left|\frac{\alpha}{\Delta l}\right|^2\sigma_{\Delta l}^2 + 2\left|\frac{1}{S_{21}\Delta l}\right|^2\sigma^2_{|S_{21}|}, \tag{20}$$

$$\sigma_\beta^2 = \left|\frac{\theta}{\Delta l^2}\right|^2\sigma_{\Delta l}^2 + 2\left|\frac{1}{\Delta l}\right|^2\sigma^2_{\phi S_{21}}. \tag{21}$$

These equations have been calculated by taking Eq. (12) and following the same procedure made in Eq. (17).

In order to cover all cases, using S-parameters and line length errors, a Monte Carlo simulation has been performed. The lines defined in the previous section, whose length was 10 and 35 mm respectively, were used. The standard deviations were set to $\sigma_{|S|} = 0.1$ dB, $\sigma_{\phi S} = 5°$ and $\sigma_{\Delta l} = 0.02$ mm and errors were generated using a Gaussian distribution [18]. Figures 3 and 4 show the influence of the magnitude and phase error for each of the methods. As can be seen, there is a resonant behavior in Methods 1 and 3. The resonances in Method 1 are located at the points $(n-1)\lambda = \Delta l$, while in Method 3 are located at $\left(\frac{n-1}{2}\right)\lambda = \Delta l$, for $n =$ 1,2,3…However, there is a greater variance in Method 3 than Method 1. On the other hand, Method 2 works in a completely different way, because σ_α^2 is constant in frequency with the magnitude error and 0 with the phase error, as expected in the ideal case shown in Eq. (20). Furthermore, the variance obtained using Eq. (20) is the same to the one shown in Figs. 3 and 4. It is also important to mention that this is the only method that allows negative solutions for the attenuation constant, because only the positive square root solutions in Eq. (14) are considered.

Regarding the phase constant, Figs. 3 and 4 depicts how magnitude and phase error affect it. As seen, the effect produced is quite similar to the one of the attenuation constant. Note that what is plotted is not the phase constant itself, but the unwrapped one. This is because mathematical software usually take just the principal value (first solution for $n = 0$) in Eq. (16). That solution is between $\beta = \pm\pi/\Delta l$ and have no physical sense, as β increases with frequency. For this reason, a phase unwrap of $\beta \cdot \Delta l$ must be performed to obtain the estimated value of β. The unwrap function works great when there are no errors. However, when random errors are

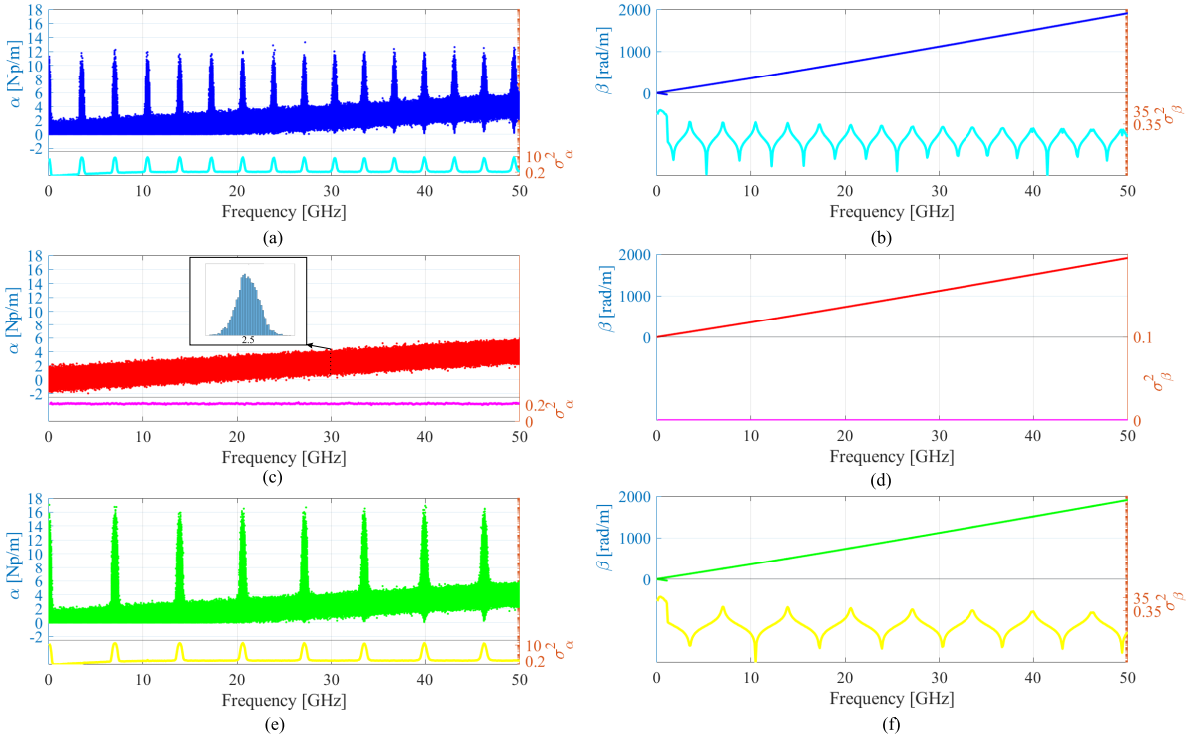

FIGURE 3. Attenuation and phase constants and their variances obtained by using $\sigma_{|S|} = 0.1$ dB through Method 1: (a), (b), Method 2: (c), (d), Method 3: (e), (f).

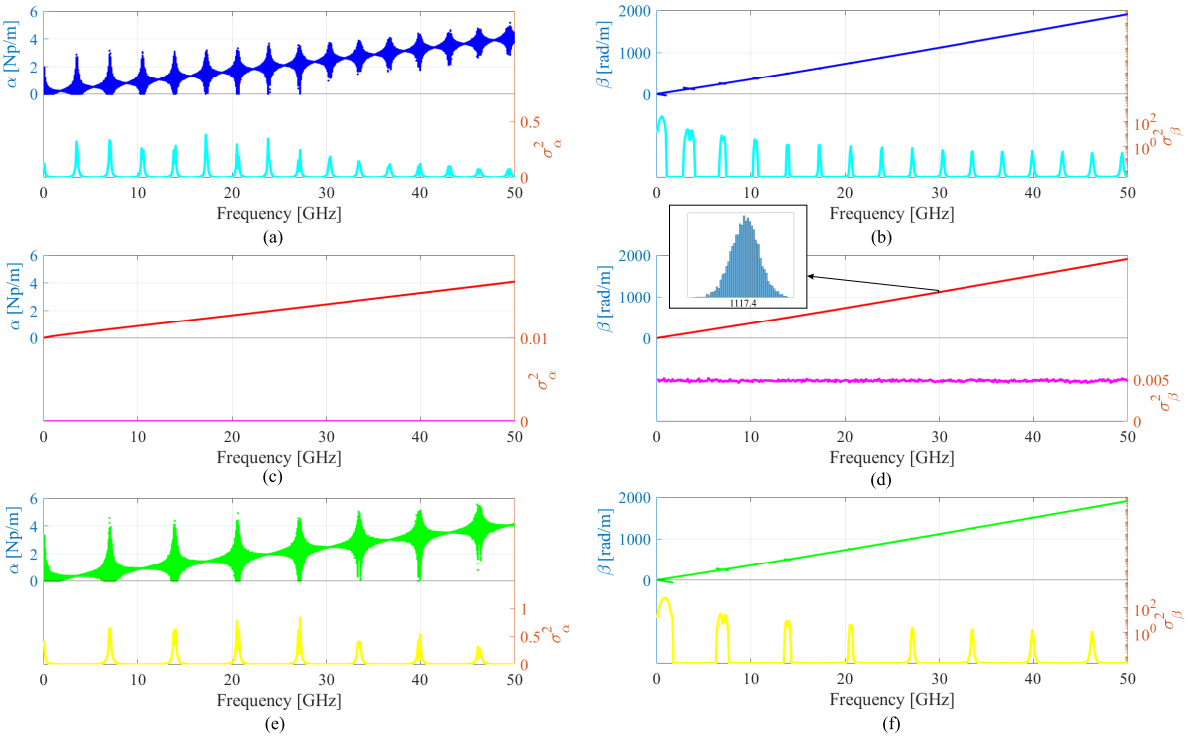

FIGURE 4. Attenuation and phase constants and their variances obtained by using $\sigma_{\phi S} = 5°$ through Method 1: (a), (b), Method 2: (c), (d), Method 3: (e), (f).

introduced, it may occur that the function picks an incorrect solution. This effect is more significant at very low frequency, when the value of the phase constant is lower.

Finally, Fig. 5 show the influence of line length error. Only Method 1 results are plotted, as they are equal to those obtained through Methods 2 and 3. As expected in

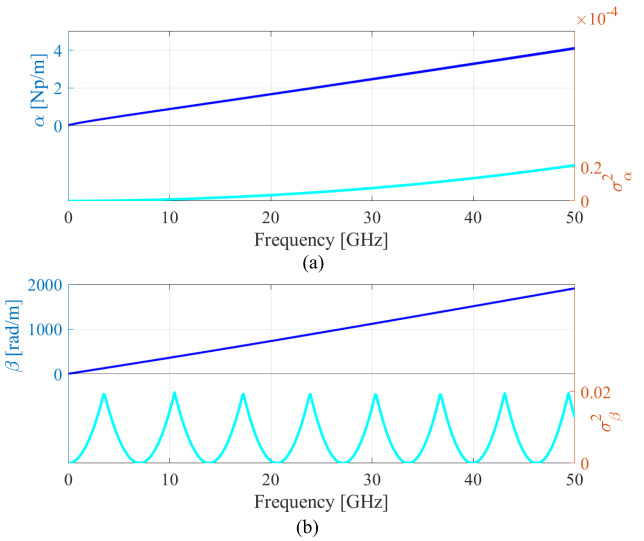

FIGURE 5. Attenuation (a) and phase (b) constants and their variances obtained by using a line length variance $\sigma_{\Delta l} = 0.02$ mm through Method 1.

Eqs. (18) and (19), this error results in a bias in the solution, and the variance increased with α^2 and θ^2. However, it must be taken into account that, because of the unwrap behavior previously mentioned, the maximum and minimum values of θ are $\pm\pi/\Delta l$ respectively, so the value of σ_β^2 will be limited. The performance of the sensitivity analysis has been validated through T-tests, showing that the attenuation and phase constants have a Gaussian distribution. In addition, and to show them, two histograms have been depicted in Figs. 3 and 4.

IV. MINIMIZATION APPROACH

A. OVER DETERMINATION OF THE METHODS

The presence of random errors means that it is not possible to determine the exact value of the propagation constant, so the objective is to achieve the best estimation from available measurements. In the previous section, it has been demonstrated how these errors affect the different methods examined in this work. To improve the accuracy of the methods, it is proposed to increase the number of lines to be measured and use a least squares estimation. Thereby, the effects produced by random errors in measurements are minimized as the Least-Mean-Square (LMS) is the maximum likelihood estimator. The propagation constants can be obtained by solving the equations:

1) Method 1:

$$\min_{\alpha,\beta} \frac{1}{2}\sum_{n=1}^{N}\left|\text{trace}([M]) - \left(e^{+\gamma\Delta l} + e^{-\gamma\Delta l}\right)\right|^2, \quad (22)$$

2) Method 2:

$$\min_{\alpha,\beta} \frac{1}{2}\sum_{n=1}^{N}\left|\left(\frac{1/\lambda_1 + \lambda_2}{2}\right) - e^{+\gamma\Delta l}\right|^2, \quad (23)$$

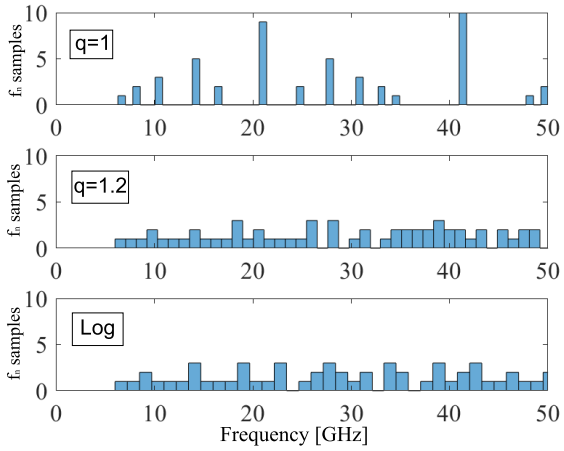

FIGURE 6. Histograms of f_n for different line length distributions.

3) Method 3:

$$\min_{\alpha,\beta} \frac{1}{2}\sum_{n=1}^{N}\left|\left(\frac{\det([M_{1+2}])}{\det([M_1])} - 2\right) - \left(e^{+\gamma\Delta l} + e^{-\gamma\Delta l}\right)\right|^2, \quad (24)$$

where N is the number of possible combinations between all the k lines, taken two by two. The measurements of S-parameters of N lines, $N > 2$, get to M simultaneous non-linear complex equation. The value of M is given by the combinations of N lines taken 2 at a time: $M = 1/2 \cdot N(N-1)$. Increasing slightly the number of lines, the total number of combinations increase rapidly and so, the number of estimations of the propagation constant is also increased. In the experiment that has been carried out, a number of seven lines has been used, providing 21 combinations of two lines taken at a time. Increasing N is a reasonable way to reduce uncertainty, but this increment should be accompanied by different Δl values, to achieve better results. Optimal line lengths selection will be explored in the next section.

B. OPTIMAL LINE LENGTHS

One of the most important parts to reduce random errors is the choice of the lengths of the lines employed. The length distribution must be chosen so that the differences between the increments in the length of the lines should be as small as possible. In addition, the bigger the increments, the better. Constant increments in length between different transmission lines concentrate resonances in discrete number of frequency points. Small deviations from that pattern spread the resonances through the band of interest. The selected lengths can follow a quasi-linear distribution

$$l_i = l_0 + \Delta L\left(\frac{i-1}{N-1}\right)^q, i = 1, 2, \ldots N, \quad (25)$$

or a logarithmic one

$$l_i = l_0 + \Delta L\frac{\log\left(l_0 + \frac{i-1}{N-1}\Delta L\right) - \log(l_0)}{\log(l_N) - \log(l_0)}, \quad i = 1, 2, \ldots N, \quad (26)$$

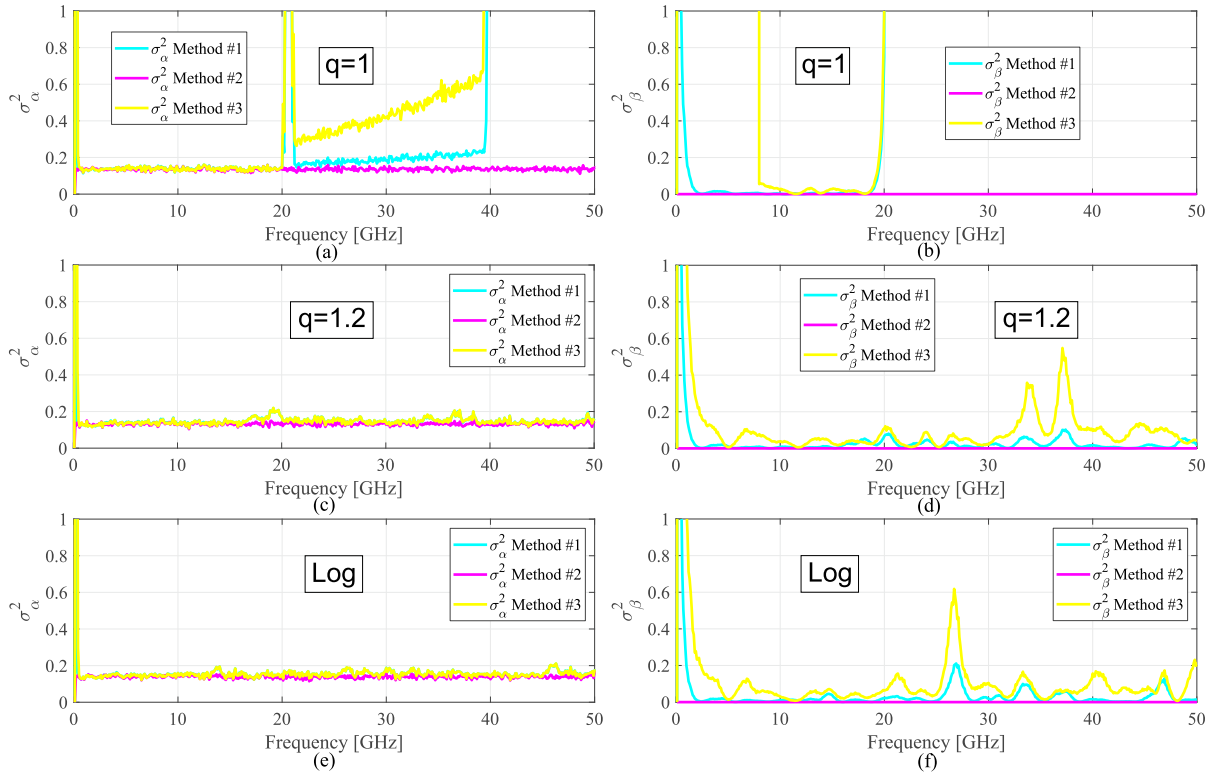

FIGURE 7. Attenuation and phase constants variances obtained for $\sigma_{|S|} = 0.1$ dB and the three proposed methods using a linear criteria (a), (b), quasi-linear criteria (c), (d) and logarithmic criteria (e), (f).

where l_0 is the shortest line length, l_N is the longest, and $\Delta L = l_N - l_0$. In the quasi-linear one, the factor q just need to be adjust to a value different of 1 (that is the linear distribution). The frequencies where the phase difference of measured S_{21} is zero can be easily obtained from

$$f_n = \frac{n \cdot c}{\Delta l \sqrt{\varepsilon_{\mathrm{r,eff}}}}. \tag{27}$$

Figure 6 compares histograms of the aggregation of frequencies where the phase difference between measured S_{21} appears. As seen, $q = 1.2$ and the logarithmic one are the most homogeneous distribution through the frequency band, whereas $q = 1$ still shows a resonant behavior. Furthermore, as the resulting covariance improves with larger length increments, the quasi-linear distribution has those increments and will be the one chosen to perform the experimental validation of the methods.

C. RESULTS

In order to assess how over determination affects random errors, the experiment shown in Section III has been repeated using 7 lines instead of 2. To choose the line lengths, the three distributions set out in Fig. 6 were used. The minimum (l_0) and maximum (l_N) line lengths are set to 10 and 35 mm respectively. All line lengths are depicted in Table 1.

Figures 7 and 8 show the variances of the attenuation (σ_α^2) and the phase (σ_β^2) constants respectively for the aforementioned length strategies and the three proposed methods. In these figures, the standard deviations were set to $\sigma_{|S|} = 0.1$ dB and $\sigma_{\phi S} = 5°$, the same values used in Section III, in order to evaluate the improvements produced by the over determination of the methods. As seen, the fact of increasing the number of lines significantly reduces errors in the propagation constant. On the one hand, the values of σ_α^2 and σ_β^2 are less than the ones using 2 lines. On the other hand, the resonant behavior has disappeared when the two non-linear length strategies are employed. By using these strategies, the results of Methods 1 and 3 are considerably improved, and can be comparable to the ones of Method 2. Furthermore, and as expected, quasi-linear and logarithmic strategies work in a similar way.

Regarding the length error, Fig. 9 shows the resultant variance of the propagation constant after applying the proposed over determination of the methods to the aforementioned 7 lines. For this plot, the standard deviation of the length has been set again $\sigma_{\Delta l} = 0.02$ mm. The results are considerably better than the ones in Fig. 5, when the methods were applied to 2 lines. Furthermore, it is important to mention that, again, the linear distribution maintains a resonant behavior, whereas the quasi-linear and the logarithmic ones work in a similar way.

V. REAL CASE METHOD ASSESSMENT BY MEASUREMENTS

The developed theory has been tested using circuital simulations in the previous sections. To validate it experimentally, a set of 7 lines made of Rogers RO4350B has been

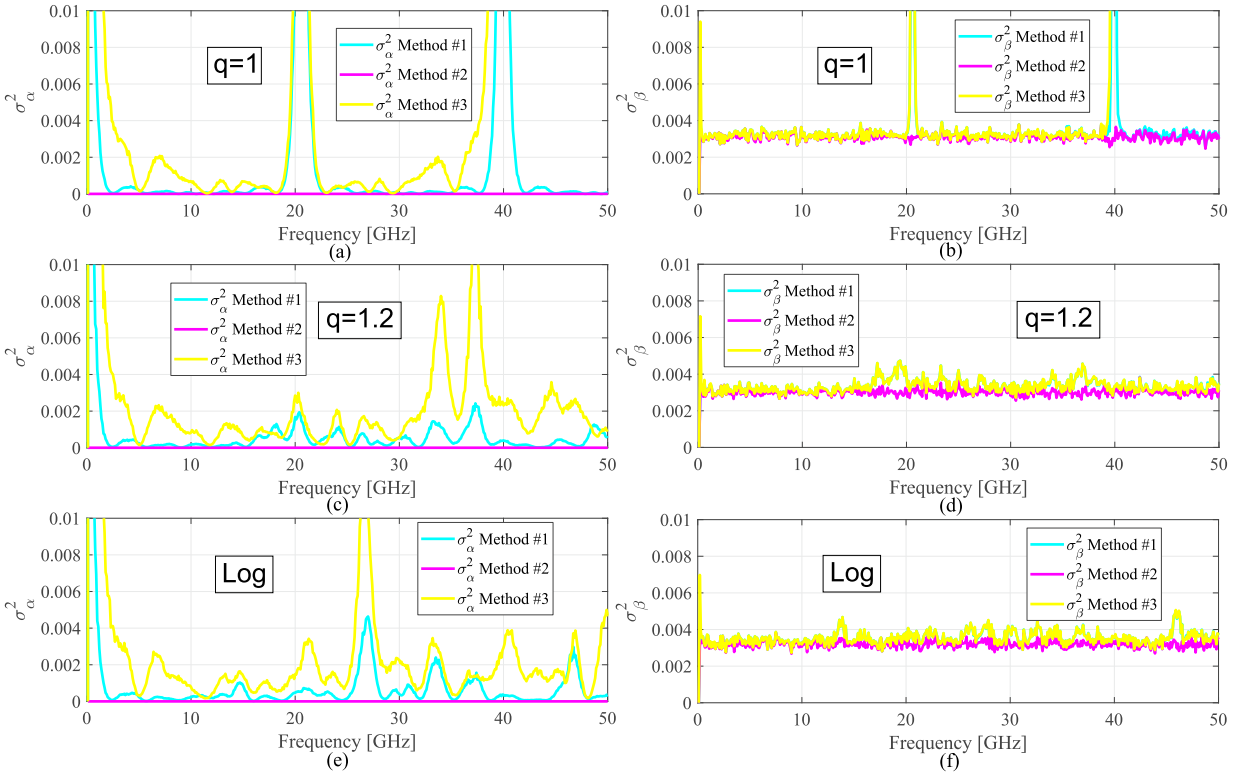

FIGURE 8. Attenuation and phase constants variances obtained for $\sigma_{\phi S} = 5°$ and the three proposed methods using a linear criteria (a), (b), quasi-linear criteria (c), (d) and logarithmic criteria (e), (f).

TABLE 1. Line lengths using different cutting strategies.

Length strategy	l_1 (mm)	l_2 (mm)	l_3 (mm)	l_4 (mm)	l_5 (mm)	l_6 (mm)	l_7 (mm)
Linear	10	14.16	18.33	22.50	26.66	30.83	35
Quasi-linear ($q = 1.2$)	10	12.91	16.69	20.88	25.37	30.09	35
Logarithmic	10	16.95	22.09	26.18	29.57	32.47	35

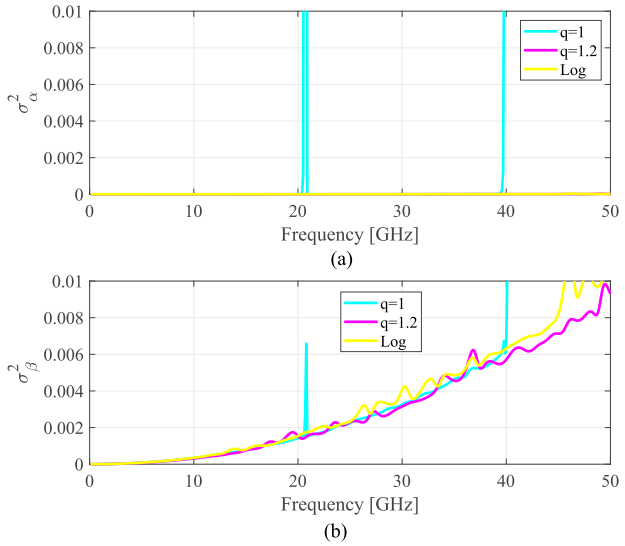

FIGURE 9. Attenuation (a) and phase constants (b) variances obtained for $\sigma_{\Delta l} = 0.02$ mm and the three proposed methods.

manufactured. This material, whose permittivity and dispersion are known and given by the manufacturer [19], will be used to assess the methods performance. This frequency-dependent permittivity is imported into the full-wave simulator ANSYS HFSS, to obtain a more realistic and accurate simulation that can be compared with the experimental results. Considering that similar results are obtained when using a quasi-linear or a logarithmic distribution, the first one ($q = 1.2$) has been chosen to design the line lengths. These lengths are depicted in Table 1. S-parameters of the 7 lines are taken by using the network analyzer Agilent PNA-X (N5247A), between 0.01 and 50 GHz. A photograph of the real measurement setup is shown in Fig. 10. Figure 11 depicts the simulated and measured results of the structure. The phase constant, β, has been plotted in terms of effective relative permittivity, $\varepsilon_{\mathrm{r,eff}}$, in order to reduce the range of possible values and to make easier to extract information from the graph. For this purpose, the variance of the effective relative permittivity can be obtained from the transformation

$$\sigma^2_{\varepsilon_{\mathrm{r,eff}}} = \sigma^2_\beta \left| \frac{\partial \varepsilon_{\mathrm{r,eff}}}{\partial \beta} \right|^2 = 2\sigma^2_\beta \frac{c^2}{\omega^2} \beta. \tag{28}$$

The confidence intervals shown in Fig. 11 have been calculated from Eqs. (20) and (21). S-parameter magnitude and phase variances have been extracted from the analyzer datasheet [20], whereas length variance has been chosen by taking 10 measures of the same line with a digital caliper, and calculating the variance of these measurements, that was $\sigma^2_{\Delta l} = 0.02$ mm. As it can be seen, the confidence intervals

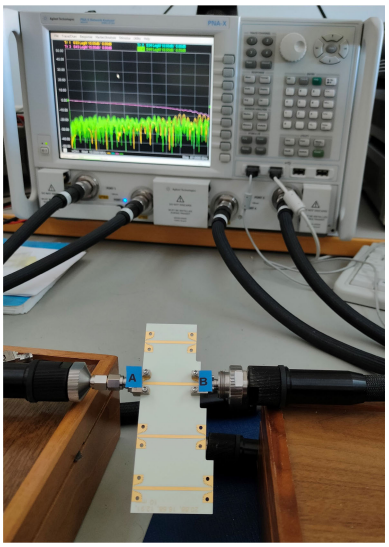

FIGURE 10. Photograph of microstrip lines and the measurement setup using vector network analyzer for S-parameters measurement.

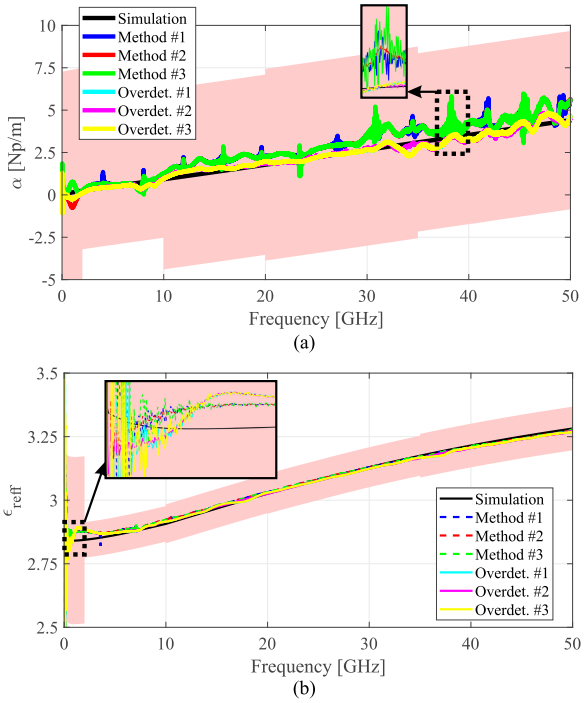

FIGURE 11. Experimental results of the attenuation (a) and phase (b) constants using the proposed methods with 2 and 7 lines, in comparison with electromagnetic simulation.

are discontinuous in frequency. This is due to the fact that the analyzer manual specifies S-parameter variances for different frequency ranges, so shifts in confidence intervals are located in the frequency points in which an interval change occurs in the analyzer, being more noticeable in the attenuation constant.

As seen in Fig. 11, both the 2-lines and the 7-lines results are within the confidence intervals. The attenuation constant obtained by taking 2 lines shows quite well the difference between the three proposed methods. Method 1 displays a resonant behavior in more frequencies than the rest. However, these resonances are noisier when happening in Method 3, whereas Method 2 is the most insensitive to errors. However, it is important to mention that the over determination of the three methods eliminates most of the noise and makes the measured attenuation constant quite similar to the one obtained through electromagnetic simulation. The same reasoning can be applied to the effective relative permittivity. Specifically, in the lower frequencies it is possible to see that both Method 1 and 3 are much noisier than Method 2. However, the methods are much more accurate for estimating the phase constant. This is mainly due to the fact that the phase variance of the analyzer is much smaller than the magnitude one. Despite this, the experimental results show an excellent agreement with the simulated ones, which points out the use of this kind of over determined methods for the estimation of the propagation constant.

VI. CONCLUSION

In the present work, we have studied how three different methods used for the experimental characterization of the propagation constant of transmission lines are affected by random errors. Although it might be thought that these three methods work in a similar way, it has been demonstrated that they have a totally different behavior in presence of random measurement errors. Specifically, the method based on eigenvalues is the one that shows better tolerance to errors, while the other two have resonant behaviors. For this reason, it is considered the best option to use an eigenvalue-based method to calculate the propagation constant when only two-line measurements are available. In order to reduce errors in the propagation constant, the proposed over determination of the methods, based on a least-squares approximation, works better when the number of lines is increased. Furthermore, resonant behavior can be eliminated by using the proposed non-linear length selection criteria. If it is taken, all the methods work in a similar way regarding random errors. Finally, the developed analysis carried out has been corroborated by comparing electromagnetic simulations with uncalibrated real measurements, showing an excellent agreement between both attenuation and phase constants between simulated and measured results up to 50 GHz. In addition, experimental results have shown that the behavior of the methods is different in presence of errors, and that it is improved substantially when the proposed over determination is applied.

APPENDIX A
METHOD EQUATIONS AS FUNCTION OF S-PARAMETERS

In this section, the analytical equations of the three proposed methods are expressed as a function of the S-Parameters. For this purpose, $\delta^{(n)}$ must be taken as $S_{12}^{(n)}S_{21}^{(n)} - S_{11}^{(n)}S_{22}^{(n)}$ and $\chi = \delta^{(1)}+\delta^{(2)}+S_{11}^{(1)}S_{22}^{(2)}+S_{11}^{(2)}S_{22}^{(1)}$, being $S^{(n)}$ the S-parameter matrix of line n.

Method 1:

$$\gamma = \frac{1}{\Delta l}\cosh^{-1}\left(\frac{\chi}{2S_{21}^{(1)}S_{12}^{(2)}}\right). \tag{29}$$

Method 2:

$$\gamma = \frac{1}{\Delta l} \ln \left(\frac{\chi - \sqrt{\chi^2 + 4\left(S_{22}^{(2)} - S_{22}^{(1)}\right)\left(\delta^{(2)} S_{11}^{(1)} - \delta^{(1)} S_{11}^{(2)}\right)}}{4 S_{21}^{(1)} S_{12}^{(2)}} + \frac{S_{21}^{(1)} S_{12}^{(2)}}{\chi + \sqrt{\chi^2 + 4\left(S_{22}^{(2)} - S_{22}^{(1)}\right)\left(\delta^{(2)} S_{11}^{(1)} - \delta^{(1)} S_{11}^{(2)}\right)}} \right). \quad (30)$$

Method 3:

$$\gamma = \frac{1}{\Delta l} \cosh^{-1} \left(\frac{\left(S_{21}^{(2)} + S_{21}^{(1)}\right)\left(\delta^{(1)} S_{21}^{(2)} + \delta^{(2)} S_{21}^{(1)}\right) + \left(S_{11}^{(1)} S_{21}^{(2)} + S_{11}^{(2)} S_{21}^{(1)}\right)\left(S_{22}^{(1)} S_{21}^{(2)} + S_{22}^{(2)} S_{21}^{(1)}\right) - 2\left(S_{21}^{(2)}\right)^2 S_{12}^{(1)} S_{21}^{(1)}}{2\left(S_{21}^{(2)}\right)^2 S_{12}^{(1)} S_{21}^{(1)}} \right). \quad (31)$$

REFERENCES

[1] M. Cauwe and J. D. Baets, "Broadband material parameter characterization for practical high-speed interconnects on printed circuit board," *IEEE Trans. Adv. Packag.*, vol. 31, no. 3, pp. 649–656, Aug. 2008.

[2] P. I. Deffenbaugh, R. C. Rumpf, and K. H. Church, "Broadband microwave frequency characterization of 3-D printed materials," *IEEE Trans. Compon., Packag., Manuf. Technol.*, vol. 3, no. 12, pp. 2147–2155, Dec. 2013.

[3] M. Perez-Escribano and E. Marquez-Segura, "Parameters characterization of dielectric materials samples in microwave and millimeter-wave bands," *IEEE Trans. Microw. Theory Techn.*, vol. 69, no. 3, pp. 1723–1732, Mar. 2021.

[4] L. Chen, C. Ong, C. Neo, V. Varadan, and V. Varadan, *Microwave Electronics: Measurement and Materials Characterization*. Hoboken, NJ, USA: Wiley, 2004. [Online]. Available: https://books.google.es/books?id=1vmUdUXlBNIC

[5] B. Bianco and M. Parodi, "Measurement of the effective relative permittivities of microstrip," *Electron. Lett.*, vol. 11, no. 3, pp. 71–72, Feb. 1975.

[6] V. Rizzoli, "Resonance measurement of single- and coupled-microstrip propagation constants," *IEEE Trans. Microw. Theory Techn.*, vol. MTT-25, no. 2, pp. 113–120, Feb. 1977.

[7] W. Kim, S. Hee Lee, M. Cheol Seo, M. Swaminathan, and R. R. Tummala, "Determination of propagation constants of transmission lines using 1-port TDR measurements," in *59th ARFTG Conf. Dig. Spring*, Jun. 2002, p. 6.

[8] A. M. Nicolson and G. F. Ross, "Measurement of the intrinsic properties of materials by time-domain techniques," *IEEE Trans. Instrum. Meas.*, vol. IM-19, no. 4, pp. 377–382, Nov. 1970.

[9] K.-F. Fuh, "Broadband continuous extraction of complex propagation constants in methods using two-line measurements," *IEEE Microw. Wireless Compon. Lett.*, vol. 23, no. 12, pp. 671–673, Dec. 2013.

[10] G. F. Engen and C. A. Hoer, "Thru-reflect-line: An improved technique for calibrating the dual six-port automatic network analyzer," *IEEE Trans. Microw. Theory Techn.*, vol. MTT-27, no. 12, pp. 987–993, Dec. 1979.

[11] R. B. Marks, "A multiline method of network analyzer calibration," *IEEE Trans. Microw. Theory Techn.*, vol. 39, no. 7, pp. 1205–1215, Jul. 1991.

[12] J. A. Reynoso-Hernandez, "Unified method for determining the complex propagation constant of reflecting and nonreflecting transmission lines," *IEEE Microw. Wireless Compon. Lett.*, vol. 13, no. 8, pp. 351–353, Aug. 2003.

[13] Y. Rodriguez-Velasquez, S. C. Sejas-Garcia, and R. Torres-Torres, "A method of differences for determining the propagation constant from multiline measurements," *IEEE Microw. Wireless Compon. Lett.*, vol. 30, no. 3, pp. 300–303, Mar. 2020.

[14] C. Wan, B. Nauwelaers, W. D. Raedt, and M. Van Rossum, "Two new measurement methods for explicit determination of complex permittivity," *IEEE Trans. Microw. Theory Techn.*, vol. 46, no. 11, pp. 1614–1619, Nov. 1998.

[15] J. van Heuven and T. Rozzi, "The invariance properties of a multivalue n-port in a linear embedding," *IEEE Trans. Circuit Theory*, vol. CT-19, no. 2, pp. 176–183, Mar. 1972.

[16] D. A. Frickey, "Conversions between S, Z, Y, H, ABCD, and T parameters which are valid for complex source and load impedances," *IEEE Trans. Microw. Theory Techn.*, vol. 42, no. 2, pp. 205–211, Feb. 1994.

[17] M. D. Janezic and J. A. Jargon, "Complex permittivity determination from propagation constant measurements," *IEEE Microw. Guided Wave Lett.*, vol. 9, no. 2, pp. 76–78, Feb. 1999.

[18] A. Lewandowski, W. Wiatr, and D. Williams, "Multi-frequency approach to vector-network-analyzer scattering-parameter measurements," in *Proc. 40th Eur. Microw. Conf.*, Sep. 2010, pp. 260–263.

[19] *Ro4000 Series High Frequency Circuit Materials*. Accesed: 2021. [Online]. Available: https://rogerscorp.com/-/media/project/rogerscorp/documents/advanced-connectivity-solutions/english/data-sheets/ro4000-laminates-ro4003c-and-ro4350b—data-sheet.pdf

[20] (2021). *Keysight 2-Port and 4-Port PNA-X Network Analyzer*. [Online]. Available: https://literature.cdn.keysight.com/litweb/pdf/N5247-90002.pdf

MARIO PÉREZ-ESCRIBANO (Graduate Student Member, IEEE) was born in Alcalá la Real, Jaén, Spain, in December 1993. He received the B.S. degree in telecommunication engineering from the University of Málaga, Málaga, Spain, in 2015, and the M.S. degree from the University Carlos III de Madrid, Madrid, Spain, in 2017. He is currently pursuing the Ph.D. degree with the Departamento de Ingeniería de Comunicaciones, Escuela Técnica Superior de Ingeniería (E.T.S.I.) de Telecomunicación, Universidad de Málaga, Málaga.

In 2014, he joined the Departamento de Ingeniería de Comunicaciones, Escuela Técnica Superior de Ingeniería (E.T.S.I.) de Telecomunicación, Universidad de Málaga. In 2019, he did a research stay at the NASA Jet Propulsion Laboratory, USA. His research interests include the analysis of structures made by additive manufacturing techniques, planar circuits, and dielectric resonator antennas.

Mr. Pérez-Escribano was a recipient of the Spanish Ministry of Education, Culture and Sports Scholarship for the term 2017–2022.

ENRIQUE MÁRQUEZ-SEGURA (Senior Member, IEEE) was born in Málaga, Spain, in April 1970. He received the Ingeniero de Telecomunicación and Doctor Ingeniero degrees from the Universidad de Málaga, Málaga, in 1993 and 1998, respectively.

In 1994, he joined the Departamento de Ingeniería de Comunicaciones, Escuela Técnica Superior de Ingeniería (E.T.S.I.) de Telecomunicación, Universidad de Málaga, where he became an Associate Professor, in 2001. His current research interests include electromagnetic material characterization, additive manufacturing, measurement techniques, and RF, microwave, and millimeter wave circuits design for communication applications.

Dr. Márquez-Segura was a recipient of the Spanish Ministry of Education and Science Scholarship for the term 1994–1995.